Chapter 8
Thermosalient Phenomena in Molecular Crystals: A Case Study of Representative Molecules

Yoshinori Yamanoi, Kenichiro Omoto, Toyotaka Nakae, and Masaki Nishio

Abstract Molecular crystals have a regularly packed structure, and their physical properties often depend on intramolecular and intermolecular interactions. Here, we review the crystal jumping phenomena under a thermal stimulus (thermosalient phenomenon). Thermosalient phenomena are characterized by thermal phase transitions and anisotropic lattice expansion/contraction at a microscopic scale and jumping behavior through bending/deformation/rotation/cleavage of crystals at a macroscopic scale. The absence of strong intermolecular interaction in the crystal and the misalignment of the crystal plane associated with the phase transition are explained as factors causing the thermosalient phenomena. In this chapter, various case studies with representative molecular crystals that exhibit the thermosalient phenomenon are explained in detail.

Keywords Thermosalient phenomena · Jumping crystals · Phase transitions · Polymorphism

8.1 Introduction

Some molecular crystals are known to change their physical properties on mechanical stimulation or exposure to solvent vapor. Such crystals, whose packing arrangement and physical properties change in conjunction with weak external stimuli, are called "soft crystals," and they have attracted considerable attention recently [1]. When a crystal is heated, it generally melts and becomes a liquid. However, some crystals

Y. Yamanoi (✉) · K. Omoto · T. Nakae · M. Nishio
Department of Chemistry, The University of Tokyo, Bunkyo-Ku, Tokyo 113-0033, Japan
e-mail: yamanoi@chem.s.u-tokyo.ac.jp

K. Omoto
Division of Materials Science, Nara Institute of Science and Technology (NAIST), Ikoma, Nara 630-0101, Japan

T. Nakae
Department of Applied Chemistry, Tokyo Metropolitan University, Hachioji, Tokyo 192-0397, Japan

M. Kato and K. Ishii (eds.), *Soft Crystals*, The Materials Research Society Series,
https://doi.org/10.1007/978-981-99-0260-6_8

exhibit jumping phenomena through distortion, deformation, and cleavage of crystals with phase transition. These were referred to as terms such as “jumping crystals” or “hopping crystals”. Gigg et al. named these crystals that convert thermal stimuli into mechanical motion “thermosalient crystals” (salient: meaning “jumping”), and the term is now well established [2]. Approximately 60 “thermosalient crystals” have been reported by 2021. The characteristics of thermosalient crystals are as follows: they exhibit (1) first-order phase transition, (2) similar crystal packing before and after the phenomenon, (3) no change in space group and a little change in lattice parameters, (4) anisotropic lattice size change, and (5) negative coefficient of thermal expansion in one axis direction at least. Some reviews related to the thermosalient phenomenon have been reported so far [3, 4]. However, this research is a new field and there are many unknown aspects. The definition is not unified, and there are some exceptions which do not observe the characteristics ((1)–(5)) mentioned above.

Although the mechanism of the thermosalient phenomenon is still unclear, it has been pointed out the relation with the martensitic dislocation (transformation) observed in shape memory alloys [5, 6]. The shape memory alloy forms a square lattice in the high-temperature phase. At low temperatures, the crystal packing changes to a folding screen shape due to shear deformation, in which the rhombic lattice shifts maintaining the linkage with adjacent atoms through the slip plane (Fig. 8.1). Molecular crystals showing thermosalient phenomenon exhibit a similar response to martensitic dislocations and have displacement motion against the slip plane without strong interaction in the crystal. When volume and/or shape changes occur in the original crystal structure through a phase transition, the accumulated stress (strain) is rapidly released near the lattice defect, and the crystal exhibits a mechanical response with deformation or cleavage along the slip plane. In an ordinary crystal, the deformation and cleavage proceed slowly, and the external shape gradually changes. On the other hand, the crystals exhibiting thermosalient phenomenon are characterized by the generation of instantaneous mechanical power that causes the crystals to jump.

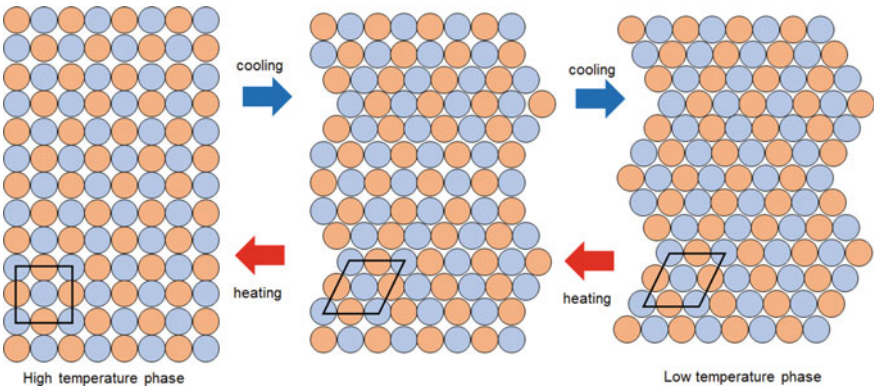

Fig. 8.1 Schematic diagram of a martensitic dislocation

8.2 Analytical Methods for Thermosalient Phenomena

The thermosalient phenomenon is generally mainly observed visually on a temperature variable plate. The phenomenon is considered to be caused by an accidental rapid structural change from the metastable phase to the stable phase of the crystal with changes in temperature, and often requires observation time in the range of several milliseconds to several seconds. Therefore, observation with a high-speed camera on a temperature-controlled stage is a useful method for instantaneously capturing crystal deformation and jumping behavior and linking microscopic phenomena to macroscopic shape changes. The phenomenon is confirmed by analytical chemistry methods such as temperature-variable X-ray diffraction and thermal analysis. Basically, the temperature of the phase transition and the temperature showing the thermosalient phenomenon are almost the same. The differential scanning calorimetry (DSC) of the molecules that exhibit thermosalient phenomenon results in the saw-toothed or jagged peaks. One of the reasons for this phenomenon is that the timing of the accidental structural change from the metastable to stable crystal packing is affected by the crystal size and/or shape.

8.3 Thermosalient Phenomena in Crystals Classified Based on Crystal Characteristics and Mechanism of the Thermosalient Phenomena

The thermosalient phenomena depend on molecular structure, and the visually observed phenomena can be classified into jumping, rotation, fragmentation, explosion, cracking, and splitting. In fact, the mechanical response is caused by a mixture of these phenomena, and the jumping distance is several mm to several cm, which is larger than the crystal size. The thermosalient phenomenon is often exhibited by organic crystals or complex crystals with weak intramolecular interaction, intermolecular interaction, steric hindrance, and high flexibility.

In 2013, Naumov conducted a systematic analysis of the thermal analysis, kinetic properties, and crystal structures of ca. 10 compounds that exhibited thermosalient phenomena at that time. They classified the compounds into three classes: crystals of flat rigid molecules aggregated in sheets (class I crystals), Crystals of molecules with bulky substituents attached to a cyclic core group (class II crystals), and crystals of molecules with extended intermolecular hydrogen bonds (class III crystals) [7–10]. During the last decade, many other crystals exhibiting thermosalient behaviors have been found. Although it is not easy to classify them clearly into Naumov's three categories, we will explain representative molecules as case studies referring to the classification.

8.3.1 *Crystals of Flat Rigid Molecules Aggregated in Sheets (Class I Crystals)*

The characteristic of this type molecules is the formation of layered structure through π–π stacking and dipole interaction in the crystalline state. Crystals are anisotropically slid and released as mechanical motion when strains that exceed the interlayer interaction are accumulated by thermal stimulation. Typical molecules of class I crystals are shown in Fig. 8.2.

1, 2, 4, 5-Tetrabromobenzene **1** forms a layered packing structure through the interaction between Br···Br and Br···H; however, it shows a tendency to form contact

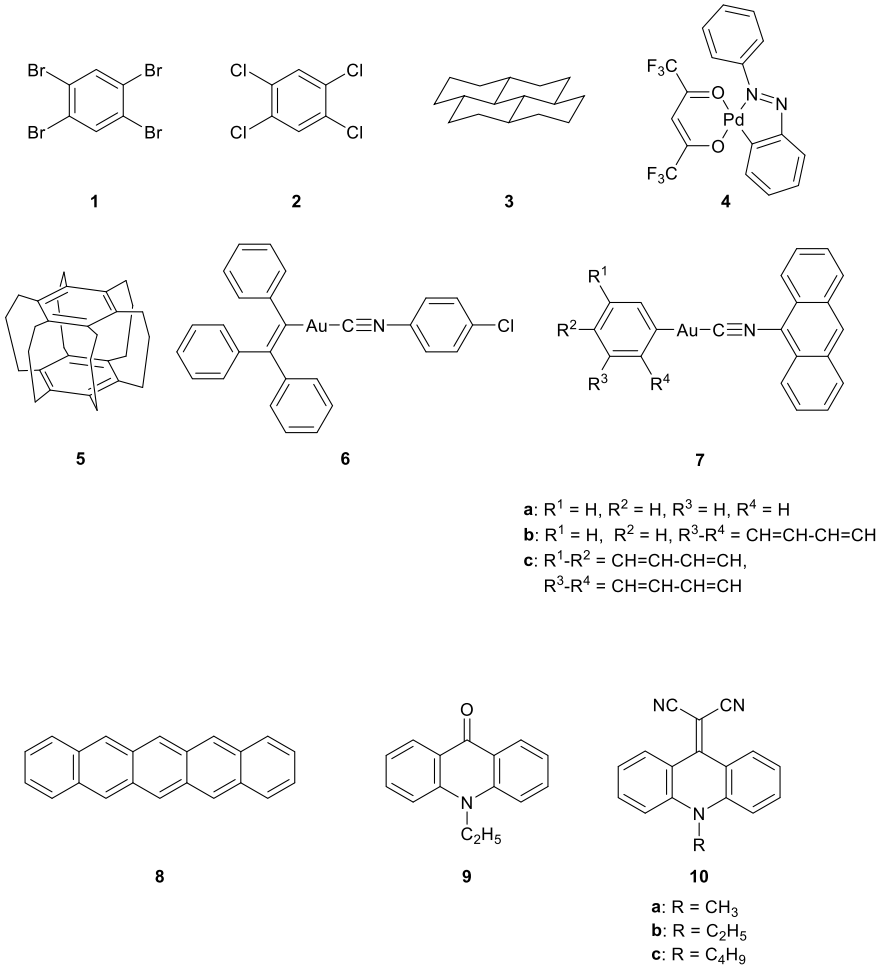

Fig. 8.2 Representative examples of molecules that create class I crystals

twins with respect to the (110) crystalline plane. Crystals of compound **1** have a stable β phase at room temperature and a stable γ phase at > 46 °C. Naumov et al. studied the direction and motion for more than 150 crystals with heating [11, 12]. They observed that the crystals are cleaved along the twin plane when heated parallel to the twin plane, and are crushed when heated perpendicular to the twin plane. Both β and γ phases have a layered structure, and the crystal jumping phenomenon is governed by the interaction between Br…Br and CH…Br. Comparing the two structures, the crystal lattice stretches anisotropically during the phase-to-phase transition. The angle between adjacent aromatic rings changes from 22.6° in β phase to 13.7° in γ phase. This slight change in inclination causes the flattening of the entire sheet-like structure, and the strain is finally accumulated and converted into mechanical behavior through cleavage and rupture [13]. Similarly, crystals of 1,2,4,5-tetrachlorobenzene **2** exhibit a thermosalient phenomenon by the mechanism as **1**, but it shows thermosalient phenomenon at a lower temperature (around 200 K) [14].

Crystals of hexadecahydropyrene **3** exhibit a crystal jump phenomenon when heated above 71.5 °C and when cooled below 65.5 °C, respectively [15]. Hexadecahydropyrene **3** has a chair-shaped conformation and is layered and packed parallel via van der Waals interactions. Because the crystals after the phase transition sublimate, X-ray structure analysis has not been successful. Although we cannot discuss the mechanism in detail, the molecule slides in the layer and strain is accumulated due to the displacement of the crystal plane under heating. The internal stress is relaxed at the transition point (e.g., lattice defect), and crystal cleavage is induced from the slip plane, resulting in a crystal jumping.

Crystals of palladium complex **4** were already known to exhibit thermosalient phenomenon in 1983 [16], but was investigated in detail by Naumov et al. [17]. This molecule has five polymorphs. A reversible phase transition occurs between the α and β phases. The stacked sheet-like structures separate from each other, as the layers between the molecules slide against each other and the molecular arrangements decline. At this time, a crystal jumping phenomenon is observed. The γ crystal undergoes a phase transition to the β crystal at 369 K. In this case, the alternating layers slide in opposite directions to form a head-to-tail stacking structure, which is transformed into a thermodynamically stable β crystal.

[3.3.3.3.3.3](1,2,3,4,5,6)-Cyclophane (superphane, **5**) are hexa-bridged cyclophanes in which all aromatic carbons of the benzene dimer are linked by propylene spacers. This compound was first synthesized by Virgil Boekelheide in 1979 as a model compound for the investigation of physical properties including aromaticity. This compound shows a crystal jumping phenomenon when heated [18]. Although the single-crystal structure at low temperature has been reported [19], the structural analysis at high temperature and the mechanism of the crystal jumping phenomenon are not well understood.

Seki and Ito et al. analyzed the crystal jumping phenomenon associated with the phase transition of triphenylethynyl 4-chlorophenyl isocyanide gold(I) complex **6** at around −40 °C with a high-speed camera (Fig. 8.3) [20]. In this crystal, a sheet-like structure is formed through π–π stacking structure. A phase transition is observed in the crystal lattice upon cooling, and the crystal lattice expands and contracts

anisotropically. The misalignment of the π–π stacking and Au–Au bonds in the packing induces deformation and cleavage of the crystal, which leads to thermosalient phenomena before and after the phase transition.

Further developing this study, crystals of (9-isocyanoanthracene)gold(I) complex **7** exhibit thermosalient and photosalient (crystal jumps due to light irradiation) phenomena in response to two different external stimuli (UV irradiation and cooling) [21]. On cooling, the crystal contracts anisotropically without changing the chemical structure. The X-ray structure analysis at 20 °C and −140 °C shows that the distance between Au…Au in the stacked dimer changes from 3.6714−3.6124 Å. Correspondingly, the crystal lattice anisotropically expanded and contacted. In contrast, the anthracene moiety is photodimerized and the structure changes significantly under UV irradiation. These changes are the reason for the salient phenomenon. The crystal shows a continuous mechanical response by alternating cooling and UV irradiation.

Pentacene **8** has four polymorphs in single crystal and thin film [22]. In the single-crystal state, pentacene **8** has a herringbone packing with an interplanar distance d_{001} = 1.41 nm in the low-temperature phase. A phase transition occurs around 486 K (high-temperature phase, Campbell phase) with a change in the interplanar distance to d_{001} = 1.44 nm [23, 24]. The angle between the molecular long axis and the normal to the *ab*-plane is 24.2° and 24.6° in the low-temperature phase changes to 21.0° and 22.5° in the high-temperature phase. Cracking and jumping of the crystal during the crystalline phase transition are reported, but no detailed analysis has been performed.

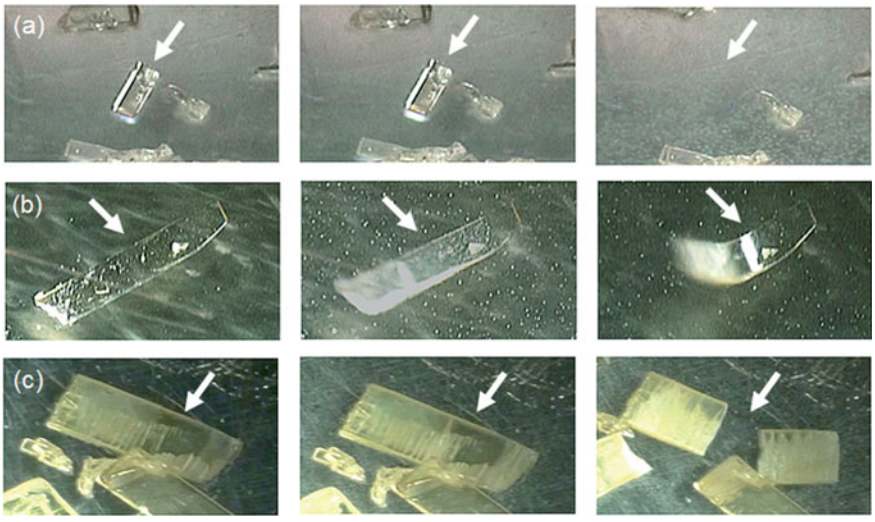

Fig. 8.3 High-speed camera observation of crystals of molecule **6** in a cooling process. The arrows indicate the points of change, **a** jumping, **b** bending, and **c** cleavage. From reference [20]. Copy right © 2019 Royal Society of Chemistry

Takeda and Akutagawa reported that crystals of ethylacridone **9** and dicyanomethylenated acridones **10** show thermosalient phenomena [25]. Especially for **10**, they investigated the molecules with different lengths of alkyl groups introduced on the nitrogen. Among them, only **10a**, **10b**, and **10c** showed the thermosalient phenomenon. Although these molecules have a bent structure, they have intermolecular interactions between C≡N···H–C(sp^2) and C≡N···H–C(sp^3). Hence, they adopt a stacked layered structure. They are considered to exhibit molecular inversion and thermosalient phenomena. When the alkyl chain becomes long, the thermosalient phenomenon is not exhibited. It is considered to be because the fluctuation of the alkyl chain becomes larger than the inversion of the ring structure under heating.

8.3.2 Crystals of Molecules with Bulky Substituents Attached to a Cyclic Core Group (Class II Crystals)

Crystals classified as class II are composed of molecules with bulky and flexible substituents attached to a cyclic core. Conformational changes of flexible substituents in crystals result in crystal-to-crystal thermal phase transition with anisotropic change in the unit cell. Accumulated strain energy is converted into mechanical motion. In some cases, crystal structures of class II thermosalient crystals have not been clarified, making it difficult to explain the mechanism of their mechanical behaviors. Representative examples of molecules that provide class II thermosaliant crystals are shown in Fig. 8.4.

Oxitropium **11** bromide is an anticholinergic drug used in the treatment of bronchial asthma and chronic obstructive pulmonary disease [26]. Block-like crystals prepared from methanol and methylene chloride show crystal jumping phenomenon upon heating up to 45 °C and cooling down to 27 °C, respectively. When this crystal is heated, the rigid aza-tricyclic moiety shows little conformational change, whereas the conformations of the ester moiety and phenyl ring are altered, causing a crystal-to-crystal phase transition. The resulting anisotropic cell expansion and packing switches induce cleavage and jumping of crystals [27].

Crystals of the sugar alcohol derivative (±)-3,4-di-*O*-acetyl-1,2,5,6-tetra-*O*-benzyl-*myo*-inositol **12** have long been known to exhibit a thermosalient phenomenon. Crystal structural analysis at variable temperature revealed **12** has three polymorphic forms (I, II, and III), which exhibit thermal phase transition at 30 °C (I → II)、70 °C (II → III), 40 °C (III → II), and 11 °C (II → I) respectively. In the case of phase transition between II and III, the occupied volume of a molecule in the crystals changes by approximately 2% resulting in a thermosalient phenomenon [28]. Whereas in the case of transition between I ⇄ II, the change of occupied volume of a molecule is smaller (approximately 1.4%). Although the molecular packing in each crystal is similar, the drastic change in the torsion of the flexible C–O–CH_2–C_6H_4 moiety (especially positions 1 and 5) work as a key

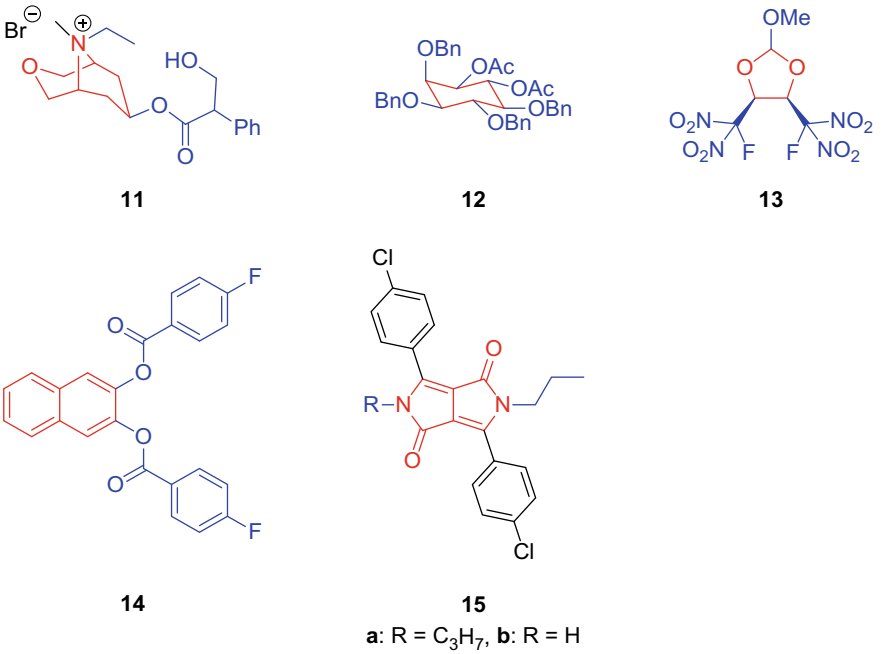

11 **12** **13**

14 **15**

a: R = C_3H_7, **b**: R = H

Fig. 8.4 Representative examples of molecules which create class II crystals. The cyclic cores are shown in red, and the bulky and flexible substituents are shown in blue

role to realize crystal-to-crystal phase transition with the thermosalient phenomenon (Fig. 8.5).

Crystals of 4,5−bis(fluorodinitromethyl)−2−methoxy−1,3−dioxolane **13** have been reported to crack and jump up to approximately 1 cm upon heating to 40 °C on a glass plate [29]. Single crystal X-ray structure analysis revealed that in crystal,

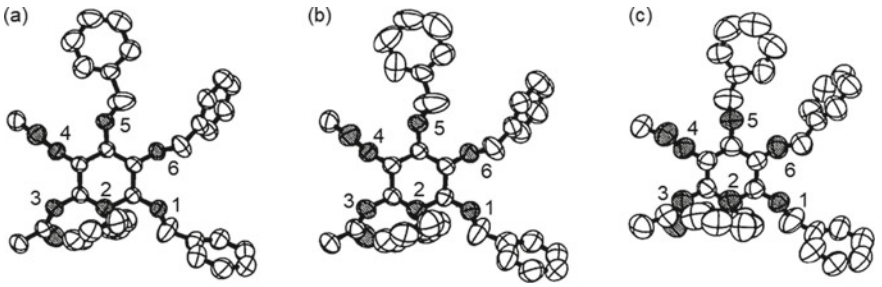

Fig. 8.5 Conformational changes of the molecule **12** before and after the phase transition. Numbers from 1 to 6 represent the position of the benzyloxy and the acetyl groups. **a** Form II, 18 °C. **b** Form II, 60 °C. **c** Form III, 80 °C. From reference [28]. Copy right © 1993 International Union of Crystallography

(1) the 1,3-dioxolane ring of the core of **13** is slightly twisted, (2) **13** constructs a layered structure parallel to the *bc* plane, and (3) the distance between the nitro group O···O is as short as 2.9 Å within layers. No detailed discussion about the correlation between structure and the thermosalient phenomenon was provided.

The diester molecule **14** with a naphthalene moiety as a core has five polymorphic forms (I–V). Among them, a reversible crystalline phase transition accompanied with a thermosalient phenomenon is observed in the transition between crystals I and IV. Crystal structures of these two polymorphs revealed that the reversible tweezering motion of the flexible diester arms of **14** induces crystal-to-crystal thermal phase transition accompanying with the thermosalient phenomenon [30].

Matsumoto et al. reported that diketopyrrolopyrrole **15a** has two polymorphic forms which exhibit a thermal phase transition with a thermosalient phenomenon. [31, 32] In the crystal of phase I, **15a** forms a one-dimensional chain packing (space group: *P*-1) through Cl···Cl interactions and π-stacking. On the other hand, upon heating of the crystals up to around 440 K, crystals transit to phase II in which **15a** forms a herringbone-type packing (space group $P2_1/c$) without any specific intermolecular interaction. Significant conformational changes of propyl and *p*-chlorophenyl groups are observed before and after thermal phase transition, which may have an important role to realize the thermosalient phenomenon. Moreover, crystals of **15b** also exhibit a thermosalient phenomenon which accompanies conformational change of the flexible propyl group during phase transition [33].

8.3.3 Crystals of Molecules with Extended Intermolecular Hydrogen Bonds (Class III Crystals)

Molecules classified in this group have hydrogen bonding sites, such as carboxyl, amide, and hydroxyl groups, etc. on their backbones, which create hydrogen bonding networks in crystals. For crystals to exhibit thermosalient phenomena, these hydrogen-bonded networks must have a two-dimensional or one-dimensional structure, and these assemblies must be packed with weak intermolecular interactions. Upon temperature change, thermal phase transition accompanying cooperative sliding of hydrogen-bonded assemblies proceeds in crystals, and the resulting strain energy converts into mechanical motion. Representative examples of molecules that provide class III crystals are shown in Fig. 8.6.

In crystal, terephthalic acid **16** forms intermolecular hydrogen-bonded carboxyl dimers at both carboxyl groups on its phenyl ring to develop two-dimensional infinite sheet-like structures which stack along [001] direction. As shown in Fig. 8.7, **16** forms two polymorphic forms: Form I, in which hydrogen-bonded carboxyl dimer in one layer locate just above that in the adjacent layer, and Form II, in which hydrogen-bonded carboxyl dimer in one layer locate above phenyl ring of **16** in the adjacent layer. Upon heating crystals, Form II crystals exhibit phase transition at around 90–95 °C and convert into Form I. The stress applied during this thermal phase transition

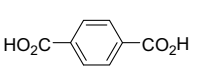

16

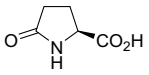

17

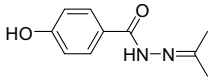

18

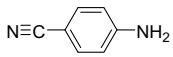

19

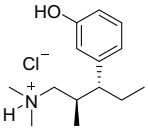

20

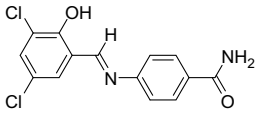

21

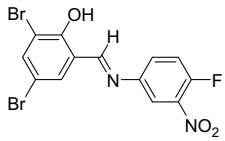

22

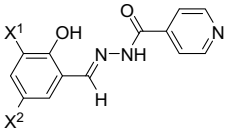

23

a: X^1 = Cl, X^2 =Cl
b: X^1 = Cl, X^2 =Br
c: X^1 = Br, X^2 = Br
d: X^1 = I, X^2 = I

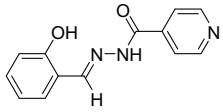

24

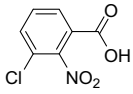

25

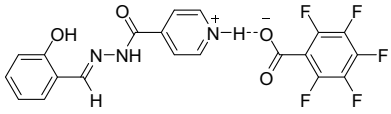

26

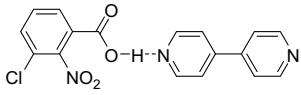

27

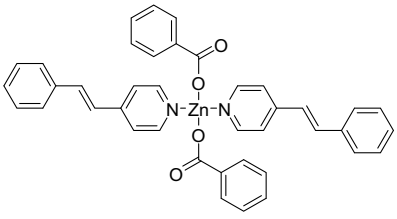

28

Fig. 8.6 Representative examples of molecules that create class III crystals

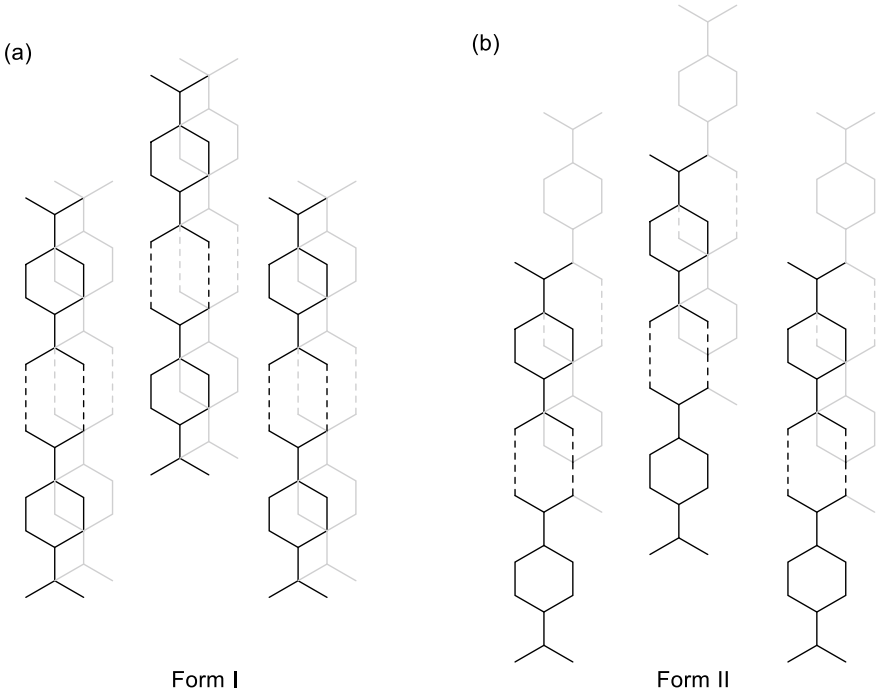

Fig. 8.7 Schematic presentation of the crystal packing of terephthalic acid **16**. The dotted lines indicate hydrogen bond, and the gray lines indicate the underlying sheet-like structure

is converted into mechanical energy to realize crystal jumping behavior. This thermal phase transition is reversible and has been observed upon cooling of Form I crystals down to 30 °C to revert to Form II [34].

L-pyroglutamic acid **17** forms a low-dimensional (one) hydrogen bonding network in crystals, which exhibit a thermosalient phenomenon associated with phase transitions [11, 35]. Large changes in hydrogen bonding (N–H···O) distances and angles have been observed before and after the phase transition. The crystals of enantiomeric D-pyroglutamic acid also shows a thermosalient phenomenon, while the racemic crystal is inert and does not exhibit crystal-to-crystal thermal phase transition.

Single crystals of *N*-2-propylidene-4-hydroxybenzohydrazide **18** exhibit single-crystal-to-single-crystal thermal phase transition among three different phases (Phase I–III) of the same space group ($Pna2_1$). Phase I is a metastable state and undergoes a phase transition via Phase II to a more stable Phase III. The phase transition from Phase I to Phase II is irreversible and proceeds at 147 °C. During this phase transition, the *c*-axis shows drastic contraction (15%), and the single crystals fragment and scatter violently [36]. Notably, the crystal fragments jump up to 1 m from their initial position. The transition between Phase II and III is reversible and does not

involve crystal jumping. The molecule exhibits second harmonic generation (SHG), the intensity of which changes before and after the phase transition.

Crystals of 4-aminobenzonitrile **19** show a thermosalient phenomenon around 180 K. This molecule forms a one-dimensional strand in a head-to-tail fashion via hydrogen bonding between N–H···N≡C in crystals. Each strand interacts with only one adjacent layer via NH…π interactions [37]. In addition, this double layer forms a crystal packing via CH···π(C≡N) interactions. Comparison of single crystal structures of **19** at 180 K and 160 K revealed a significant difference in unit cell angle (β) and the orientation of the CH···π(C≡N) interaction between two phases, indicating shearing translation of adjacent layer parallel to (100) during thermal phase transition.

Gaztañaga et al. reported that crystals of tapentadol hydrochloride **20** show a reversible first-order phase transition with the remarkable movement of samples upon heating up to 318 K and cooling down to 300 K [38]. Single-crystal structural analysis of phases I and II revealed that **20** develops hydrogen bonding parallel to the *a*-axis in crystals. Notably, there is a significant difference in the orientation of the methyl group at the end of the main alkyl chain of **20** between phases I and II, which induces a significant change in the length of the *b*- and *c*-axes and the angle of β during thermal phase transition.

Nangia et al. reported the thermosalient phenomenon of crystals of 4-((3,5-dichloro-2-hydroxybenzylidene)amino)benzamide **21** involving the C–Cl···O (halogen bond) and N–H···O (hydrogen bonds) [39]. The crystal polymorphs, Form I, Form III, and Form IV are layered, and Form II is packed in a wave-like structure. In the case of Form I and Form III, when the crystal is heated, the heat is transferred uniformly from the plane, and as a result, the thermal stress is transferred mainly in one direction, and the thermosalient phenomenon manifests as a crystal jump. On the other hand, in the case of Form II, heat transfer becomes non-uniform due to the wave-like arrangement, and it is seen that the crystal suddenly bursts.

Mishra and Ghosh et al. reported that 2-hydroxy-3,5-dibromobenzylidine-4-fluoro-3-nitroaniline **22** has two crystal polymorphic forms, one exhibiting jumping and the other exhibiting bending upon heating [40]. The differences in mechanical behaviors associated with these crystal phase transitions can be explained by the difference in conformation, packing, and intermolecular interactions of **22** in these two crystals. Crystal exhibiting jumping has a layered molecular packing via π-stacking and undergoes a phase transition with an anisotropic expansion of the cell upon heating. On the other hand, crystal exhibiting bending has an interlocked molecular packing with multiple weak and dispersive interactions and can absorb strain gradually, so that instantaneous mechanical behavior does not appear and bending behavior like bimetallic strips is realized.

Nangia et al. examined the thermosalient phenomena of crystals of halogenated salinazide derivatives **23** [41]. They discussed the effects of halogen-halogen interactions, as well as NH…N(pyridine) hydrogen bonds, on the packing structure of these molecules in crystals. Among them, crystals of **23a** exhibit a particularly pronounced thermosalient phenomenon. In this system, the weakness of the Cl···Cl interaction

is a key factor for the highly reversible phase transition accompanied by thermosalient phenomena. **23a** has three crystal polymorphic forms, Form I, II, and III; Form I and III belong to the $P2_1/c$ and Form II to the $Pca2_1$ space groups, respectively. The reversible phase transition between Form I and III shows a thermosalient phenomenon accompanied by crystal rupture. On the other hand, the phase transition from Form II to III did not involve any thermosalient phenomena.

Reddy et al. found that crystals of salinazide **24** and 3-chloro-2-nitrobenzoic acid **25** exhibit thermosalient phenomena at 130–140 °C and 210–220 °C, respectively. Moreover, co-crystals of these compounds with specific organics molecules (coformers), **26** and **27**, exhibit thermosalient phenomena at lower temperatures (at 100 °C and 100–110 °C respectively) [42]. Pentafluorobenzoic acid and 4,4'-bipyridine, which co-crystallize with **24** and **25**, do not exhibit thermosalient phenomena. The approach to developing multicomponent systems rather than single component would be promising for the preparation of libraries of thermosalient crystals to study various factors that alter the response time and temperature of thermosalient phenomenon. Moreover, proper choice of the conformer would realize additional functions such as luminescence and conductivity.

Dinnerbier, Ji and Vittal et al. reported that crystals of zinc complex **28** exhibit various properties, including thermosalient, photosalient, and SHG [43]. Single-crystal X-ray structure analysis revealed the formation of head-to-tail molecular packing structure through hydrogen bonding (C–O···H) in crystal. Upon heating, the crystals undergo a phase transition at around 140 °C without changing the space group of the crystal (C_2/c). The significant positive thermal expansion occurring along the *b*-axis of the unit lattice is due to the weakening of the π–π, CH–π, C–O···H interactions between benzoate and SPY ligands upon increasing temperature.

8.3.4 Thermosalient Phenomena Based on the Conformational Change of Flexible and Deformable Ring Structures

As examples that are difficult to classify into the above-mentioned classes (Class I–III), herein, we will discuss recently reported examples of thermosalient phenomena exhibited by crystals of cyclic molecules. Cyclic molecules have been widely studied for their potential applications in molecular recognition, catalysis, and optical materials [44, 45]. Although, conformational flexibility of cyclic compounds has been studied mainly in solution, recently there are some reports which revealed that conformational change of the cyclic molecules in crystal plays an important role in the crystal-to-crystal thermal phase transition. Designing cyclic molecules that have high crystallinity and conformational flexibility provides a clue to developing thermosalient crystals. Representative molecules are shown in Fig. 8.8.

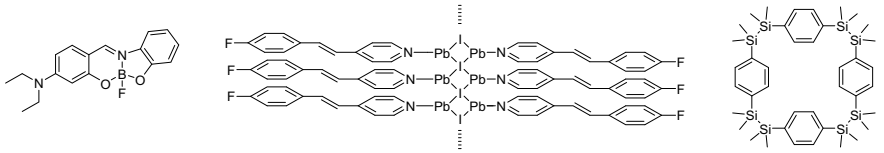

29 30 31

Fig. 8.8 Flexible and deformable cyclic molecules of crystals exhibiting thermosalient phenomena

Gon and Chujo et al. reported that a boron-fused azomethine derivative **29** has two crystal polymorphic forms (α, β) which exhibit thermosalient phenomena. In the low-temperature phase (α-type), the molecule has a nearly planar conformation, whereas in the high-temperature phase (β-type), it has a bent conformation [46, 47]. In the phase transition from α to β phase accompanied with a thermosalient phenomenon, the crystal lattice stretches anisotropically (*a*-axis ca. +10%, *b*-axis ca. +20%, and *c*-axis ca. −20%). Notably, the luminescence behavior of these crystals changes before and after the thermosalient phenomenon, and α crystal has a higher luminescence quantum yield.

Dinnebier and Vittal et al. reported that crystals of a linear 1D coordination polymer **30** composed of Pb(II) and 4-fluoro-4'-sterylpyridine exhibit a thermosalient phenomenon accompanied by structural changes in the rhombic framework of Pb(μ−I)$_2$ [48]. During the phase transition from crystalline phase I (low-temperature phase) to crystalline phase II (high-temperature phase), the aspect ratio of Pb(μ−I)$_2$ the diagonal of the rhombic skeleton changes.

The authors have synthesized a variety of disilane-bridged aromatic molecules and studied their structures and properties in crystals [49–53]. Disilane-bridged aromatic molecules have attracted much attention as building blocks of stimuli-responsive materials, because of their structural flexibility unique to σ bond and electron conjugation between σ orbital of Si–Si and π-orbitals of aromatic moiety (σ–π conjugation). So far, there are several reports about disilane-bridged aromatic molecules that exhibit stimuli-responsive polymorphism and solid-state physical properties specific to their molecular packing structures [54–56].

Recently, the authors have synthesized a rhombic disilanyl macrocycle **31** possessing four *p*-phenylenes linked by Si–Si bonds which exhibits thermal phase transition with crystal jumping and cracking [57]. Crystal structure analysis at variable temperature revealed that the disilanyl macrocycle has a rhombic structure with the disilane moiety at the apexes in both the α-form (high-temperature phase) and β-form (low-temperature phase). In the transition between α-form and β-form, the disilanyl macrocycle shows conformational transformation accompanied with a concerted parallel crank motion to change the aspect ratio of its rhombic structure. The anisotropic stretching/shrinking of the crystal lattice in the thermal phase transition induces mechanical stress resulting in crystal jumping and cracking. The bulky tetramethyldisilane structure, which suppresses π-stacking in the crystal,

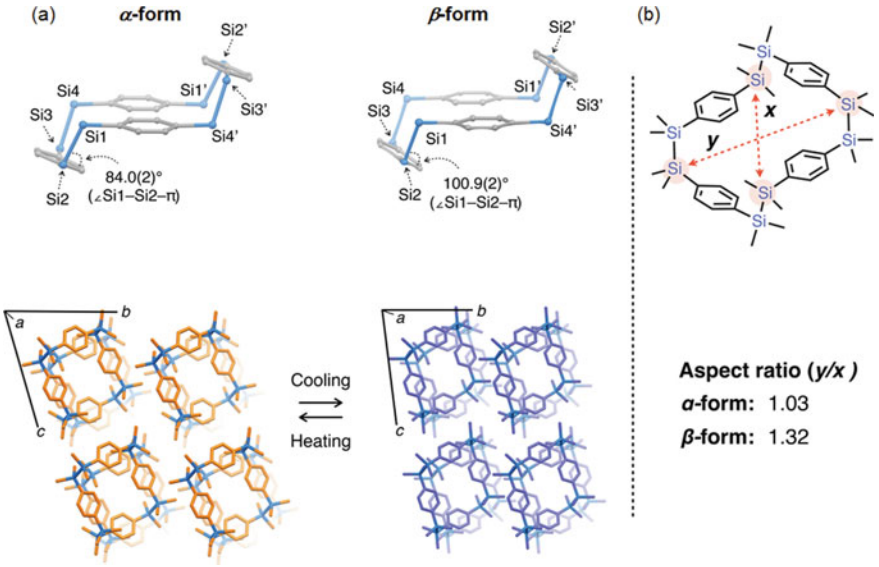

Fig. 8.9 **a** Change in the crystal structure and packing structure of the molecule **31** before and after the phase transition. **b** Change in aspect ratio of the ring structure (rhombic structure) before and after the phase transition. From ref. [57]. Copy right © 2020 American Chemical Society

seems to realize a conformational change of the disilane-based flexible skeleton of the macrocycle in the crystal (Fig. 8.9).

Garcia-Garibay, Naumov, and Rodríguez-Molina et al. [58] have reported that amphidynamic crystals of **32** composed of carbazole and DABCO (crystals with high crystallinity and fast rotation in some parts of the molecular structure) exhibit a thermosalient phenomenon (Fig. 8.10). In this crystal, four adjacent carbazole molecules create a rhombic cavity via CH···π interaction, which encapsulates DABCO via CH···N interaction. At around 320 K, a phase transition occurs from Form I to Form II as shown in Fig. 8.10, during which the rhombic cavity was deformed. From visual observation, a crystal jump phenomenon was observed from the (100) plane, which was consistent with the direction of the crystal lattice change.

8.3.5 Miscellaneous Crystals Exhibiting Thermosalient Phenomena Due to a Phase Transition

Figure 8.11 shows the molecules showing thermosalient phenomena due to the phase transition that cannot be classified in 8.3.1−8.3.4.

Xu and Raing et al. have reported that crystals of 2,7-di([1,1'-biphenyl]-4-yl)fluorenone **33** exhibit a thermosalient phenomenon [59]. In this case, it is explained

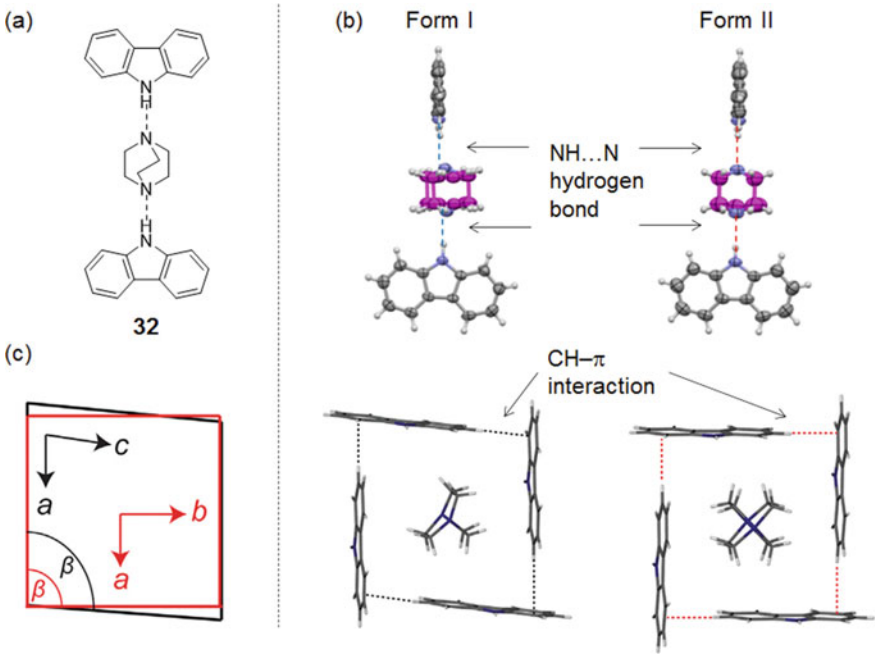

Fig. 8.10 **a** Structure of the amphidynamic crystal of **32** composed of DABCO incorporated into the rhombic structure of carbazole. **b** Phase transition of the amphidynamic crystal with DABCO incorporated into a four carbazole molecules between Form I and Form II. (c) Changes in the rhombic framework before and after the phase transition. Black: Form I. Red: Form II. From reference [58]. Copy right © 2019 Elsevier

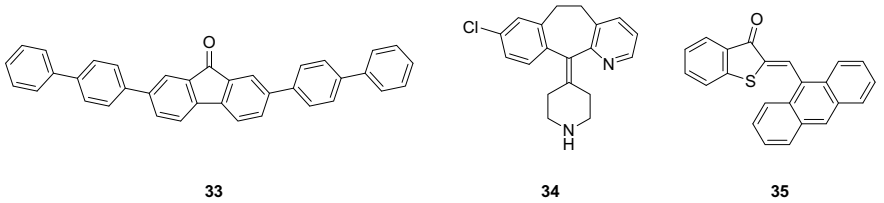

33 34 35

Fig. 8.11 Molecules of miscellaneous crystals which undergo phase transitions to exhibit thermosalient phenomena

in their report that the thermosalient phenomenon does not originate from the conformational change caused by the hindered rotation as explained in class II. The crystal phase transition and the deformation of the whole crystal are induced by the changes in the little dihedral angles among the aromatic rings located at the terminal. Anisotropic expansion and contraction of crystal lattice result in this process in crystal jumping phenomenon.

Desloratadine **34** is a common antihistamine used in the treatment of allergic reactions [60]. In the crystal, the piperidine ring in this molecule shows a ring-flipping motion resulting in phase transitions. The phase transitions of Phase I to Phase II and Phase II to Phase III occur at around 330 K and 350 K, respectively [61]. The X-ray structure analysis did not reveal any hydrogen bonding between NH···N or the formation of a two-dimensional packing structure in the crystal.

Wolf et al. studied the molecule **35** consisting of thioindiogo and anthracene [62]. When the crystals of the *Z*-form molecule are heated to 130 °C, an irreversible phase transition occurs with crystal jumping. Upon the transition, the dihedral angle between thioindigo and anthracene changes to form a *Z*'-isomer. The crystals also exhibit a photosalient phenomenon, i.e., a crystal jumping phenomenon based on the *Z-E* isomerization under UV irradiation.

Gaudon et al. reported the thermosalient phenomenon in the crystals of the inorganic compound $CuMo_{0.9}W_{0.1}O_4$ **36** [63]. With this molecule, the γ-crystal at the low-temperature forms octahedral sites with six Mo–O (W–O) bonds, whereas the α-crystal at the high-temperature forms tetrahedral sites with four Mo–O (W–O) (Fig. 8.12) [64]. A reversible thermosalient phenomenon is shown at 360 K from γ-crystal to α-crystal and at 275 K from α-crystal to γ-crystal, respectively. The γ-crystal has weak Mo–O (W–O) bonds forming molecules, while the α-crystal has higher rigidity and stronger Mo–O (W–O) bonds that crystallize with low-density packing. Thermosalient phenomenon is not observed in crystals of $CuMoO_4$, which does not contain any W. When the ratio of W to Mo is more than 0.1, it becomes a wolframite-type crystal with an octahedral structure and does not show the thermosalient phenomenon.

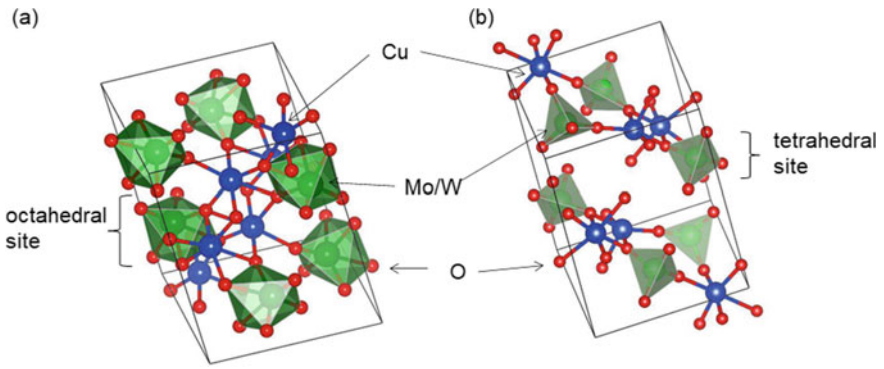

Fig. 8.12 Crystal structure of $CuMo_{0.9}W_{0.1}O_4$ **36**. **a** γ-crystal. **b** α-crystal. From reference [64]. Copy right © 2021 Elsevier

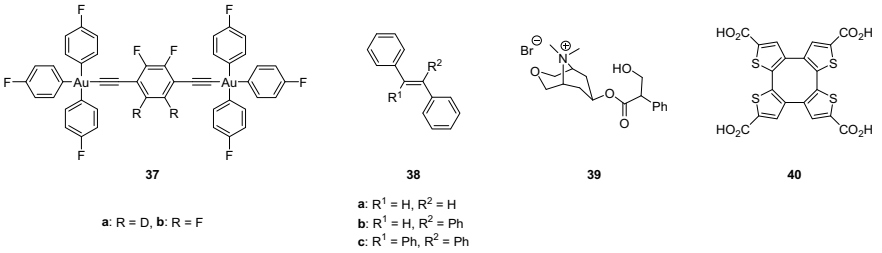

Fig. 8.13 Molecules exhibiting thermosalient phenomena without a crystal phase transition

8.3.6 Thermosalient Phenomena without Crystal Phase Transition

In this section, we introduce the thermosalient phenomenon which does not involve the crystal phase transition unlike the earlier sections. Typical compounds are shown in Fig. 8.13.

Ito and Garcia-Garibay et al. reported that crystals of dumbbell-shaped gold complexes **37** exhibit thermosalient phenomena without crystal phase transitions [65]. In this case, crystal migration and jumping phenomena are observed due to large and reversible thermal expansion with anisotropy. The luminescence behavior of these materials changes during the thermosalient phenomenon.

Seki and Ito et al. reported that crystals of a group **38** of simple hydrocarbon compounds with tetraphenylethene as a matrix skeleton exhibit a thermosalient phenomenon upon cooling to approximately −80 °C [66]. Unlike other groups of crystals, these are different crystals in which no phase transition occurs during the crystal jump phenomenon, as shown by single-crystal X-ray diffraction and differential thermal analysis. Anisotropy of thermal expansion leads to anisotropic size change of lattice parameter. Although the cause of the thermosalient phenomenon is not well understood, the approach of molecules along the direction perpendicular to the olefin plane upon cooling can be considered.

Skoko et al. have reported that crystals of methscopolamine bromide **39**, an analogue of compound **11** described in Sect. 8.3.2, exhibits a reversible thermosalient phenomenon when heated to 323–340 K and cooled to 313–303 K [67]. Although this crystal does not undergo a phase transition, it has anisotropic thermal expansion coefficients of the crystal lattice, which is the cause of the thermosalient phenomenon. Unlike the thermosalience of **11** which is derived from crystal phase transition, the crystal jumps over a wide temperature range (>10 K).

Takeda and Akutagawa reported a crystal jump phenomenon based on the adsorption and desorption of tetrahydrofuran (THF) in the channel of the hydrogen-bonded three-dimensional framework (HOF) [68] of tetra[2.3]thienylenetetracarboxylic acid **40** and the torsional motion of the ring-conjugated chain [69, 70]. The molecules of **40** form a diamond-shaped HOF. The size of the channels (vacancies) in this structure is 22.1× 23.6 Å, enclosing two THF molecules per unit. As THF is released

under heating, the core site of the tetra[2.3]thiophene skeleton undergoes a flipping motion, and the crystal lattice expands and contracts anisotropically [71]. After THF is removed, the vacancies were occupied by H_2O. This structure is transformed into the original THF-incorporated structure on exposure to THF vapor. The changes in the crystal composition and structural transformation due to the desorption of THF by heating are the causes of the thermosalient phenomenon. Although HOF is a weak structure compared to porous materials utilizing other interactions, the weak structure of HOF interestingly enables it to develop into heat-responsive materials.

Gong et al. reported the jumping behavior of crystals of a charge-transfer complex **41** that is a 1:1 co-crystal of coronene (COR; donor) and tetrafluoro-1,4-benzoquinone (TFBQ; acceptor) (Fig. 8.14) [72]. COR and TFBQ form alternating stacked crystals. The characteristic feature of this system is the utilization of TFBQ as a component, which readily volatilizes when thermally stimulated. As the temperature is gradually increased, the mechanical motion of the crystals that repeatedly flip, jump, rotate, shift, and swing is observed due to the change in crystal packing.

Shi et al. have studied the mechanical behavior of crystals of helical supramolecular metal complexes **42a** and **42b** composed of $UO_2(NO_3)_2$, dicarboxylic acid and phenanthroline (Fig. 8.15) [73]. Although no clear phase transition was observed from the temperature-variable PXRD observations, they reported that the crystals jump due to the anisotropic thermal expansion and the change in the π-stacking of the inner phenanthroline. Since the $–SO_2–$ unit in the dicarboxylic acid backbone is less sterically hindered than the $–C(CF_3)_2–$ unit, the crystal of **42b** exhibits a thermosalient phenomenon at lower temperatures.

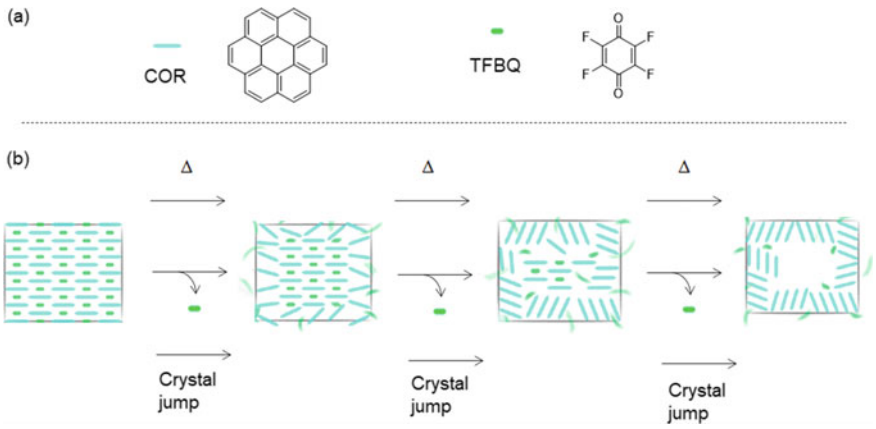

Fig. 8.14 Thermosalient phenomena utilizing components that readily volatilize upon thermal stimulation. **a** Structure of COR and TFBQ. **b** Thermally induced jumping behavior of the charge-transfer complex **41**, a 1:1 co-crystal of COR and TFBQ. From reference [72]. Copy right © 2021 American Chemical Society

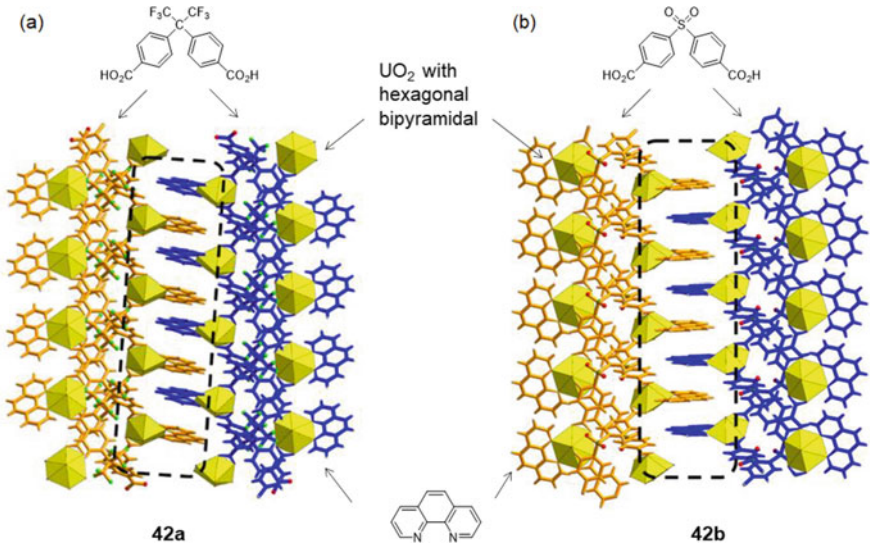

Fig. 8.15 Packing structures of supramolecular complexes **42a** and **42b** exhibiting thermosalient phenomena. From reference [73]. Copy right © 2021 Wiley–VCH

8.4 Summary

Thermosalient phenomena are caused by small changes in the arrangement of molecules in crystals in response to thermal stimuli, and manifested as fragmentation/explosion/cracking/splitting caused by changes in the crystal lattice. The constituent units of organic crystals are very simple, and it is surprising that small changes at the molecular level can be converted into macroscopic mechanical responses such as crystal jumping. The crystals exhibiting thermosalient phenomena may be used in micro-(or nano-) scale molecular machines, artificial muscles, and so on [74]. In particular, the crystal cleaves when thermosalient phenomenon occurs, which can be applied as a molecular fuse to prevent overcurrent in an electric circuit [75].

A detailed review of different type of crystals and the mechanism of the thermosalient phenomenon exhibited by them under external stimuli was provided. It is difficult to predict the crystal phase transition, the crystal polymorphism and the design of a molecule which shows the thermosalient phenomenon. Therefore, we have not yet clarified the whole picture of the thermosalient phenomenon, and various interpretations and possibilities are assumed. At present, the basic data are insufficient, and it is necessary to clarify the principle for many compounds to enable design of compounds with such properties. In this review, we introduced the salient phenomenon by thermal stimulation, and a similar phenomenon by optical stimulation (photosalient phenomenon) is also developing. For further details, another review is referred for additional information [76].

References

1. Kato M, Ito H, Hasegawa M, Ishii K (2019) Chem Eur J 25:5105–5112
2. Gigg J, Gigg R, Payne S, Conan R (1987) J Chem Soc Perkin Trans I:2411–2414
3. Seki T (2015) Kagaku to Kogyo 68:254–255
4. Takeda T (2019) Mol Sci 13:A0102
5. Porter DA, Eastering K, Sherif M (2009) Phase transformations in metals and alloys, 3rd edn. CRC Press
6. Lexcellent C (2013) Shape-memory alloys handbook. Wiley
7. Nath NK, Panda MK, Sahoo SC, Naumov P (2014) CrystEngComm 16:1850–1858
8. Commins P, Desta IT, Karothu DP, Panda MK, Naumov P (2016) Chem Commun 52:13941–13954
9. Sahoo SC, Panda MK, Nath NK, Naumov P (2013) J Am Chem Soc 135:12241–12251
10. Naumov P, Chizhik S, Panda MK, Boldyreva E (2015) Chem Rev 115:12440–12490
11. Panda MK, Runcevski T, Husain A, Dinnebier RE, Naumov P (2015) J Am Chem Soc 137:1895–1902
12. Sahoo SC, Sinha SB, Kiran MSRN, Ramamurty U, Dericioglu AF, Reddy CM, Naumov P (2013) J Am Chem Soc 135:13843–13850
13. Lieberman HF, Davey RJ, Newsham DMT (2000) Chem Mater 12:490–494
14. Karothu DP, Naumov P (2021) Isr J Chem 61:557–562
15. Ding J, Herbst R, Praefcke K, Kohne B, Saenger W (1991) Acta Cryst B47:739–742
16. Etter MC, Siedle AR (1983) J Am Chem Soc 105:641–643
17. Panda MK, Runcevski T, Sahoo SC, Belik AA, Nath NK, Dinnebier RE, Naumov P (2014) Nat Commun 5:4811
18. Takemura H (2005) Kagaku 60:46–49
19. Yasutake M, Sakamoto Y, Onaka S, Sako K, Tatemitsu H, Shinmyozu T (2000) Tetrahedron Lett 41:7933–7938
20. Seki T, Mashimo T, Ito H (2019) Chem Sci 10:4185–4191
21. Kato K, Seki T, Ito H (2021) Inorg Chem 60:10849–10856
22. Siegrist T, Besnard C, Haas S, Schiltz M, Pattison P, Chernyshov D, Batlogg B, Kloc C (2007) Adv Mater 19:2079–2082
23. Campbell RB, Robertson JM, Trotter J (1961) Acta Crystallogr 14:705
24. Campbell RB, Robertson JM, Trotter J (1962) Acta Crystallogr 15:289
25. Takeda T, Akutagawa T (2016) Chem Eur J 22:7763–7770
26. Restrepo RD (2007) Respir Care 52:833–851
27. Skoko Z, Zamir S, Naumov P, Bernstein J (2010) J Am Chem Soc 132:14191–14202
28. Steiner T, Hinrichs W, Saenger W, Gigg R (1993) Acta Cryst B49:708–718
29. Corbett JM, Dickman MH (1996) Acta Crystallogr. Sect C: Cryst Struct Commun 52:1851–1853
30. Tamboli MI, Karothu DP, Shashidhar MS, Gonnade RG, Naumov P (2018) Chem Eur J 24:4133–4139
31. So H-S, Minami T, Jindo T, Matsumoto S (2018) CrystEngComm 20:5317–5320
32. So H-S, Matsumoto S (2019) Acta Cryst B75:414–422
33. Kikuchi Y, Matsumoto S (2021) CrystEngComm 23:5882–5890
34. Davey RJ, Maginn SJ, Andrews SJ, Black SN, Buckley AM, Cottier D, Dempsey P, Plowman R, Rout JE, Stanley DR, Taylor A (1994) Mol Cryst Liq Cryst 242:79–90
35. Wu H, Reeves-McLaren N, Pokorny J, Yarwood J, West AR (2010) Cryst Growth Des 10:3141–3148
36. Centore R, Jazbinsek M, Tuzi A, Roviello A, Capobianco A, Peluso A (2012) CrystEngComm 14:2645–2653
37. Alimi LO, van Heerden DP, Lama P, Smith VJ, Barbour LJ (2018) Chem Commun 54:6208–6211
38. Gaztañaga P, Baggio R, Halaca E, Vega DR (2019) Acta Cryst B75:183–191

39. Mittapalli S, Perumall DS, Nangia A (2017) IUCrJ 4:243–250
40. Chinnasamy R, Munjal B, Suryanarayanan R, Peedikakkal AMP, Mishra MK, Ghosh S (2022) Cryst Growth Des 22:615–624
41. Mittapalli S, Perumall DS, Nanubolu JB, Nangia A (2017) IUCrJ 4:812–823
42. Rawat H, Samanta R, Bhattacharya B, Deolka S, Dutta A, Dey S, Raju KB, Reddy CM (2018) Cryst Growth Des 18:2918–2923
43. Bolla G, Chen Q, Gallo G, Park I-H, Kwon KC, Wu X, Xu Q-H, Loh KP, Chen S, Dinnebier RE, Ji W, Vittal JJ (2021) Cryst Growth Des 21:3401–3408
44. Davis F, Higson S (2011) Macrocycles: Construction, Chemistry and Nanotechnology Applications. John Wiley & Sons, Chichester
45. Liu Z, Nalluri SKM, Stoddart JF (2017) Chem Soc Rev 46:2459–2478
46. Gon M, Tanaka K, Chujo Y (2021) Chem Rec 21:1358–1373
47. Ohtani S, Gon M, Tanaka K, Chujo Y (2017) Chem Eur J 23:11827–11833
48. Rath BB, Gallo G, Dinnebier RE, Vittal JJ (2021) J Am Chem Soc 143:2088–2096
49. Nakae T, Nishio M, Yamanoi Y (2020) Bull Jpn Soc Coord Chem 76:31–39
50. Shimada M, Yamanoi Y, Nishihara H (2016) Yuki Gosei Kagaku Kyokaishi 74:1098–1107
51. Yamanoi Y (2019) Kagaku Kogyo 70:260–266
52. Yamanoi Y, Nishihara H (2009) Yuki Gosei Kagaku Kyokaishi 67:778–786
53. Yamanoi Y (2018) Keiso Kagaku Kyokaishi 35:11–17
54. Nakae T, Nishio M, Usuki T, Ikeya M, Nishimoto C, Ito S, Nishihara H, Hattori M, Hayashi S, Yamada T, Yamanoi Y (2021) Angew Chem Int Ed 60:22871–22878
55. Nishio M, Shimada M, Omoto K, Nakae T, Maeda H, Miyachi M, Yamanoi Y, Nishibori E, Nakayama N, Goto H, Matsushita T, Kondo T, Hattori M, Jimura K, Hayashi S, Nishihara H (2020) J Phys Chem C 124:17450–17458
56. Nakae T, Nishio M, Yamada T, Yamanoi Y (2021) Molecules 26:6852
57. Omoto K, Nakae T, Nishio M, Yamanoi Y, Kasai H, Nishibori E, Mashimo T, Seki T, Ito H, Nakamura K, Kobayashi N, Nakayama N, Goto H, Nishihara H (2020) J Am Chem Soc 142:12651–12657
58. Colin-Molina A, Karothu DK, Jellen MJ, Toscano RA, Garcia-Garibay MA, Naumov P, Rodríguez-Molina B (2019) Matter 1:1033–1046
59. Duan Y, Semin S, Tinnemans P, Cuppen H, Xu J, Rasing T (2019) Nat Commun 10:4573
60. DuBuske LM (2005) Expert Opin Pharmacother 6:2511–2523
61. Srirambhatla VK, Guo R, Dawson DM, Price SL, Florence AJ (2020) Cryst Growth Des 20: 1800–1810
62. Hean D, Alde LG, Wolf MOJ (2021) Mater Chem C 9:6789–6795
63. Robertson L, Penin N, Blanco-Gutierrez V, Sheptyakov D, Demourgues A, Gaudon MJ (2015) Mater Chem C 3:2918–2924
64. Pudza I, Kalinko A, Cintins A, Kuzmin A (2021) Acta Mater 205:116581
65. Jin M, Yamamoto S, Seki T, Ito H, Garcia-Garibay MA (2019) Angew Chem Int Ed 58:18003–18010
66. Seki T, Mashimo T, Ito H (2020) Chem Lett 49:174–177
67. Klaser T, Popović J, Fernandes JA, Tarantino SC, Zema M, Skoko Ž (2018) Curr Comput-Aided Drug Des 8:301
68. Lin R-B, He Y, Li P, Wang H, Xhao W, Chen B (2019) Chem Soc Rev 48:1362–1389
69. Takeda T, Ozawa M, Akutagawa T (2019) Angew Chem Int Ed 58:10345–10352
70. Takeda T, Akutagawa T (2020) Kagaku 75:66–67
71. Takeda T, Ozawa M, Akutagawa T (2019) Cryst Growth Des 19:4784–4792
72. Chen Y, Li J, Gong J (2021) ACS Materials Lett. 3:275–281
73. Mei L, An S-W, Hu K-Q, Wang L, Yu J-P, Huang Z-W, Kong X-H, Xia C-Q, Chai Z-F, Shi W-Q (2020) Angew Chem Int Ed 59:16061–16068
74. Karothu DP, Halabi JM, Li L, Colin-Molina A, Rodríguez-Molina B, Naumov P (2020) Adv Mater 32:1906216
75. Khalil A, Ahmed E, Naumouv P (2017) Chem Commun 53:8470–8473
76. Koshima H, Hasebe S, Hagiwara Y, Asahi T (2021) Isr J Chem 61:1–15